Environ Earth Sci (2016) 75:54
DOI 10.1007/s12665-015-4825-5

ORIGINAL ARTICLE

Origin of groundwater salinity and hydrochemical processes in an unconfined aquifer: case of Yang-Dai River basin in Qinhuangdao (China)

Zhenyu Sun[1,2] · **Xianfang Song**[1] · **Hongmei Bu**[1] · **Lihu Yang**[1] · **Ying Ma**[1] · **Yinghua Zhang**[1] · **Dongmei Han**[1]

Received: 9 October 2014 / Accepted: 9 July 2015 / Published online: 21 December 2015

Abstract Groundwater salinization has become a growing concern in Yang-Dai River basin of Qinhuangdao (China) where groundwater is commonly exploited for domestic, industrial and agricultural uses. In this study, hydrochemical and physical parameters of groundwater were analyzed to identify the origin of groundwater salinity and the geochemical processes occurring in the unconfined aquifer. Groundwater types are $Ca{\cdot}Mg–HCO_3{\cdot}SO_4$ in the hills, $Ca{\cdot}Mg–HCO_3{\cdot}SO_4$ in the piedmont plain and Na–Cl in the coastal alluvial plain, respectively. Electrical conductivity values varied between 322 and 3990 μS/cm. Chloride concentration attained to 942 mg/L and the proportion of seawater intrusion in the coastal alluvial plain was 5.39 % calculated by seawater fraction formal, displaying the severe seawater intrusion. Cation-exchange reactions and water–rock interactions related to the dilution of halite, gypsum, dolomite and calcite occurred by ionic relationships during seawater intrusion. High nitrate concentrations ranged from 35.6 to 686.5 mg/L distributed in the hills and the south coastal alluvial plain where they are seriously polluted by the industrial wastewater, agricultural fertilizers and domestic sewage. Seawater intrusion and nitrate contamination have common effects on the hydrochemical process in the south coastal alluvial plain. Therefore, the origin of groundwater salinization was attributed not only to seawater intrusion but also to anthropogenic pollution in the study area. This research provides useful information for groundwater salinization and water planning strategies in a coastal area.

Keywords Yang-Dai River basin · Groundwater salinity · Seawater intrusion · Nitrate contamination · Anthropogenic pollution

Introduction

Freshwater is a significant resource, and it is becoming a scarce commodity in the coastal areas where rapid population growth, intensive agriculture, prosperous tourism and industry have increased the need for freshwater resources (Trabelsi et al. 2007). In the last 30 years, groundwater salinization has become an increasing threat to the water resources in the Yang-Dai River basin. The situation is complicated due to different inputs. These include precipitation (possibly polluted or saline due to strong evaporation), seawater, ascending deep groundwater and anthropogenic sources such as wastewater or irrigation return flow (Steinich et al. 1998; Trabelsi et al. 2007).

Understanding the spatial variations in the chemical composition of groundwater is helpful to identify the different pollution sources (Mahesha and Nagaraja 1996). In the previous studies, seawater intrusion is presented as the major cause and origin of groundwater quality degradation (Xiao et al. 2014; Zhang et al. 2013). Seawater intrusion began to occur in the early 1980s and was caused by excessive exploitation of groundwater in the Yang-Dai River basin of Qinhuangdao (Han 1990). Farmland, factories and tourist areas are located on the coastal area,

---

✉ Xianfang Song
songxf@igsnrr.ac.cn

Zhenyu Sun
sunzhenyu_1209@163.com

[1] Key Laboratory of Water Cycle and Related Land Surface Processes, Institute of Geographic Sciences and Natural Resources Research, Chinese Academy of Sciences, Datun Road, A 11, Beijing 100101, People's Republic of China

[2] University of Chinese Academy of Sciences, Beijing 100049, People's Republic of China

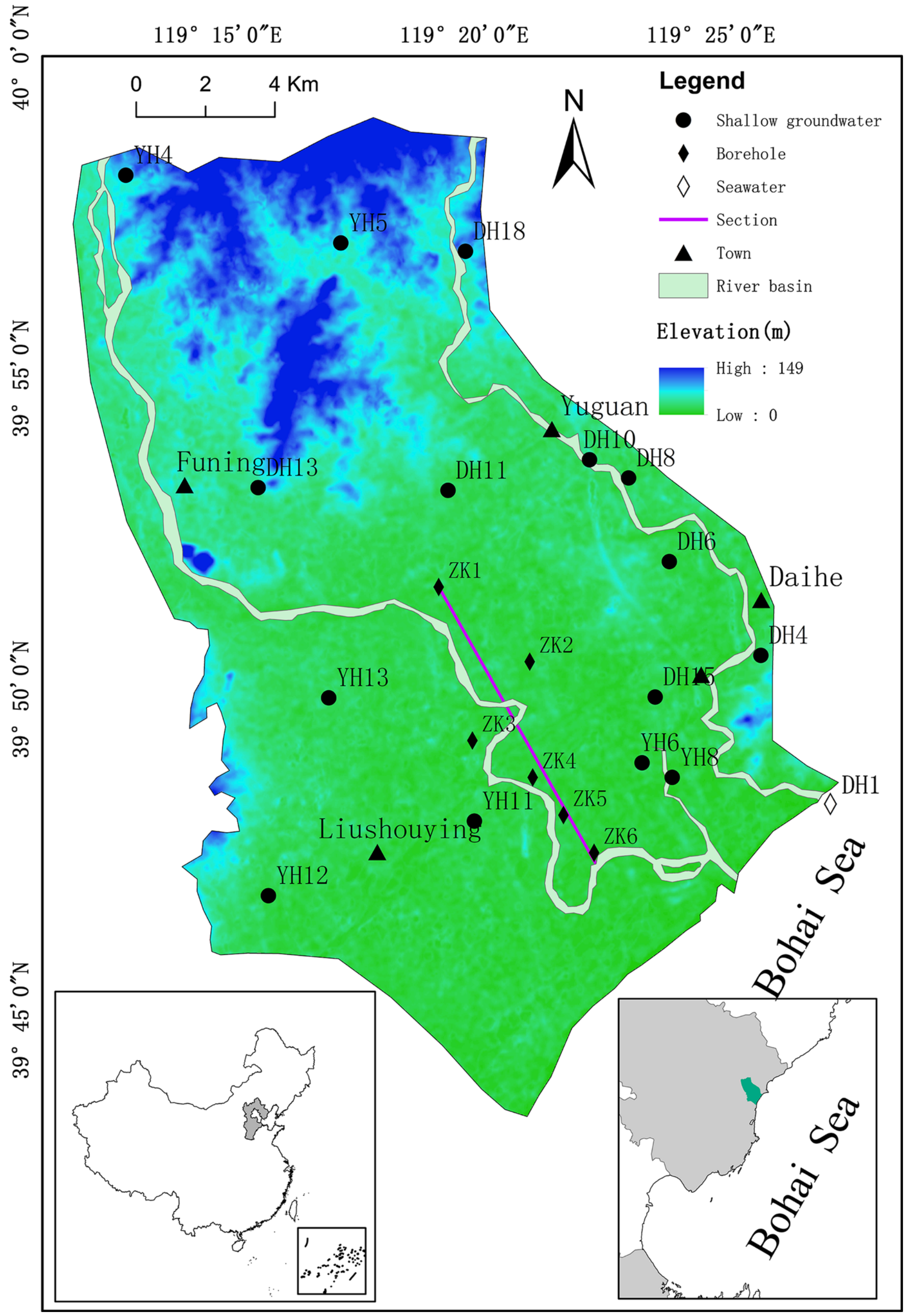

Fig. 1 Location of the study area and sampling sites

where the economy is developing rapidly. Agriculture depends on intensive irrigation and fertilization to improve the soil efficiency. Most of the fields have been covered with wheat and maize. Other crops include mainly seasonal crops such as vegetables but also apple plantations and peach orchards. Excessive amounts of fertilizers infiltrate into the groundwater with the irrigation return flow. Waste water emissions from factories (paper plants, fertilizer plants and food-processing mills) can cause deterioration of the groundwater. Furthermore, domestic sewage makes a contribution to groundwater salinization. These anthropogenic contaminations may result in high nitrate concentrations in the groundwater.

The purpose of this study is to discern the origin of the salinity (seawater intrusion or anthropogenic sources) in the unconfined aquifer using hydrochemical data. The research will contribute to adequate land and water planning strategies in the Yang-Dai River basin, as well as to preventing quantitative and qualitative alteration of the environmental conditions.

Description of the study area

The Yang-Dai River basin of Qinhuangdao is located in Northeast China along the Bohai Sea (Fig. 1) and consists of a coastal alluvial plain, a piedmont plain and a hilly area in the northwestern part of the region. It covers about 320 km^2. There are two rivers (Yang River and Dai River) in the investigated area. The climate ranges from warm temperate monsoon to coastal semi-humid climate (Zhang 2012). The mean annual precipitation is 640 mm according to the data from Qinhuangdao meteorological station, and rainfall concentrates between June and September, accounting for about 70 % of the annual precipitation (Zhang 2012).

Geology and hydrogeology

The geology of the investigated area consists of Archaeozoic gneiss, late Archean to the early Proterozoic granite and Jurassic rhyolite. The bedrock is mainly gneiss and granite. The Quaternary strata were developed by alluvial, aeolian, lacustrine and residual deposit and by artificial accumulation. It can be divided into middle Pleistocene, late Pleistocene and Holocene. Its thickness varies between 5 and 80 m and mostly concentrates between 20 and 40 m (Zuo et al. 2009).

The groundwater storage in the study area is controlled by its geological structure, stratum, lithology, topography and hydrological conditions. Abundant precipitation recharges the groundwater. The distribution of groundwater and water yield property is in tight agreement with the sedimentary environment (Fig. 2). The aquifer thickness and water yield properties show big differences in different region. The thickness of the aquifer can reach 60–70 m in the central plain and less in other areas. The groundwater can be divided into bedrock fissure water and pore water in loose rock. Bedrock fissure water can be found in the hills, and pore water in loose rock wildly distributed in the plains. The permeability deepens on lithofacies. The smaller values are attributed randomly to the less permeable lithofacies; the intermediate values are attributed to the sandstone, and the most permeable values are attributed to the sand.

Human activities

Human activities in the study area are mainly agriculture, industry and tourism. The cultivation of the fields began very early. Fertilizers that contain nutrients such as nitrogen, sulfate were used excessively to increase production. In recent years, the agricultural plant diversity increased, including vegetables, fruit plantations and greenhouse

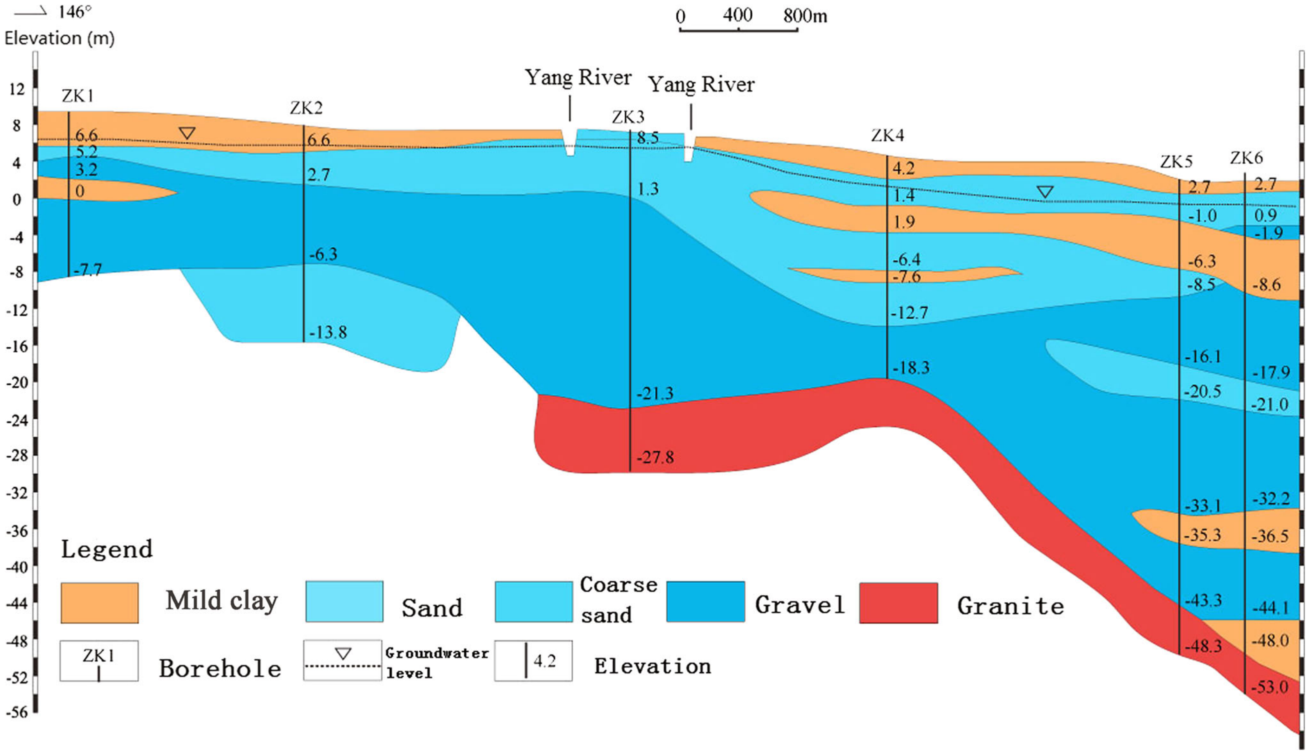

Fig. 2 Simplified geological cross section through the aquifer system (Zhang 2012)

cultivation. Numerous factories including paper mills, fertilizer plants, food-processing factories are located in the study area. A lot of waste water is released from factories which infiltrates into the groundwater. Additionally, every May to October is the peak tourist season, which also causes a threat to groundwater as it increases domestic sewage.

Materials and methods

Sample collection and treatment

Fifteen groundwater samples were taken from domestic wells in June 2013, and one seawater sample from Bohai Sea. Well location and depth were recorded when sampled, and basic information about the cropping system and land-use type surrounding the well were also recorded. Two 50-mL polyethylene bottles with watertight caps were used to store the filtered (0.45-mm millipore membrane filter) water for cations and anions analysis. All samples were stored at 4 °C after bottling.

Electrical conductivity (EC), pH and water temperature (T) were measured in situ via an EC/pH meter (WM22EP, TOA-DKK, Japan), which was previously calibrated. The HCO_3^- concentration was determined on the sampling day by titration with methyl orange as indicator and 0.01 mol/L sulfuric acid.

The major ions of the water samples were treated and analyzed in the physical and chemical analysis laboratory of the Institute of Geographic Sciences and Natural Resources Research (IGSNRR), Chinese Academy of Sciences (CAS). Cations (Na^+, K^+, Ca^{2+}, Mg^{2+}) were measured by inductively coupled plasma optical emission spectrometry (ICP-OES) (PerkinElmer Optima 5300, DV, USA). Major anion (Cl^-, NO_3^- and SO_4^{2-}) analysis was carried out by ion chromatography (IC) (Shimadzu LC-10ADvp, Japan). The detection limits for ICP-OES and IC were both 1 mg/L. Analytical precision for major ions was within 1 %. For all water samples, ion balance errors (IBE) were <10 %, and most of them were <5 %.

Methods

The seawater fraction in groundwater was estimated using chloride concentration as this ion has been considered as a conservative tracer (Custodio and Bruggeman 1987), not affected by ion exchange. It is calculated as follows (Appelo and Postma 2005):

$$f_{\text{sea}} = \frac{C_{\text{cl,sample}} - C_{\text{cl,fresh}}}{C_{\text{cl,sea}} - C_{\text{cl,fresh}}}$$

where f_{sea} is the seawater fraction, $C_{\text{Cl,sample}}$ is the Cl^- concentration of the sample, $C_{\text{Cl,sea}}$ is the Cl^- concentration of the Bohai Sea, and $C_{\text{Cl,fresh}}$ represents the Cl^- concentration of the freshwater.

The freshwater sample was chosen considering the lowest measured value of the electrical conductivity (Slama et al. 2010). The only inputs are either from the aquifer matrix salts or from a salinization source like

Table 1 In situ measurements and hydrochemical data for groundwater and seawater samples

Sample	Type	*T* (°C)	PH	EC (μS/cm)	Ca (mg/L)	Mg (mg/L)	Na (mg/L)	K (mg/L)	Cl (mg/L)	SO_4 (mg/L)	NO_3 (mg/L)	HCO_3 (mg/L)	f_{sea}% (theory)
DH4	Groundwater	21.1	7.06	322	41.73	8.218	14.17	0.66	17.79	41.13	41.72	48.17	0.00
DH18	Groundwater	22.0	6.95	515	68.56	14.73	14.07	0.67	23.73	50.24	83.55	84.29	0.03
DH13	Groundwater	17.5	6.33	528	85.29	13.97	24.06	0.80	32.22	92.06	54.24	96.90	0.08
DH10	Groundwater	19.9	6.44	624	73.01	21.35	30.19	4.98	35.41	98.15	104.68	72.82	0.10
DH11	Groundwater	16.3	6.78	648	92.62	14.34	29.07	1.40	55.86	56.62	119.45	94.61	0.22
YH13	Groundwater	22.1	6.97	1025	111.1	36.81	36.62	1.87	56.57	143.52	323.84	43.58	0.23
DH6	Groundwater	16.9	7.03	480	59.26	11.31	39.02	0.46	59.00	42.29	109.38	45.87	0.24
YH11	Groundwater	19.3	6.61	861	96.09	14.31	45.17	1.05	68.26	57.88	8.63	157.11	0.29
DH8	Groundwater	15	6.55	755	109.4	22.18	42.33	2.15	73.06	111.32	115.04	95.18	0.32
YH8	Groundwater	13.4	7.12	1126	80.55	27.04	116.2	59.21	130.51	138.04	193.1	122.13	0.66
DH15	Groundwater	21.2	6.56	1244	191	24.09	43.89	1.69	203.35	130.15	35.55	144.50	1.08
YH4	Groundwater	19.3	6.45	2270	232	89.21	123.3	2.88	275.84	286.72	686.5	132.46	1.51
YH5	Groundwater	17.1	7.31	2014	191.9	72.79	168.7	2.26	290.94	186.71	575.01	120.99	1.59
YH12	Groundwater	18.9	6.11	2200	246.6	48.72	169	4.34	322.47	210.91	559.07	120.41	1.78
YH6	Groundwater	22.3	6.21	3990	172.3	71.23	512.1	15.01	942.14	171.82	149.82	223.63	5.39
DH1	Seawater	23.6	7.55	50,000	362.8	1095	9015	340.60	17,156.43	2533.79	48.3	127.29	1.00

Table 2 Matrix of correlation coefficient for groundwater variables

	EC	Ca	Mg	Na	K	Cl	SO_4	NO_3	HCO_3
EC	1								
Ca	0.749^{**}	1							
Mg	0.853^{**}	0.811^{**}	1						
Na	0.941^{**}	0.502	0.680^{**}	1					
K	0.171	−0.088	0.071	0.271	1				
Cl	0.962^{**}	0.592^{*}	0.704^{**}	0.983^{**}	0.173	1			
SO_4	0.738^{**}	0.878^{**}	0.916^{**}	0.506	0.160	0.545^{*}	1		
NO_3	0.522^{*}	0.754^{**}	0.830^{**}	0.284	0.005	0.293	0.864^{**}	1	
HCO_3	0.786^{**}	0.569^{*}	0.533^{*}	0.766^{**}	0.251	0.798^{**}	0.450	0.116	1

** Correlation is significant at the 0.01 level (two-tailed); * correlation is significant at the 0.05 level (two-tailed)

seawater intrusion, etc. (Kouzana et al. 2009). In effect, Cl^- is not usually removed from the system due to its high solubility (Appelo and Postma 2005).

Based on the seawater fraction, the theoretical concentration of each ion i resulting from the conservative mixing of seawater and freshwater was calculated using:

$$C_{i,\mathrm{mix}} = f_{\mathrm{sea}} \times C_{i,\mathrm{sea}} + (1 - f_{\mathrm{sea}}) \times C_{i,\mathrm{fresh}}$$

where $C_{i,\mathrm{sea}}$ and $C_{i,\mathrm{fresh}}$ are the concentration of the ion i of the, respectively, seawater and freshwater.

For each ion i, the difference between the concentration of the conservative mixing $C_{i,\mathrm{mix}}$ and the measured one $C_{i,\mathrm{sample}}$ simply represents the ionic deltas resulting from any chemical reaction occurring with mixing:

$$\Delta C_i = C_{i,\mathrm{sample}} - C_{i,\mathrm{mix}}$$

When ΔC_i is positive, groundwater is getting enriched for ion i, whereas a negative value of ΔC_i indicates a depletion of the ion i compared to the theoretical mixing (Andersen et al. 2005).

Results

Hydrochemical characteristics of samples

The physical and chemical parameters of the 15 groundwater samples from the domestic wells and one seawater sample are listed in Table 1. The groundwater temperature ranges between 13.4 and 22.3 °C. The highest groundwater temperature was measured in the shallowest wells in the coastal plain, which indicates that the groundwater temperature in the wells was influenced by the high atmosphere temperature. The pH values range from 6.1 to 7.3. A part of the samples are slightly acidic, indicating an insignificant influence of the anthropogenic pollution from the irrigation return water or from industrial wastewaters (Table 2).

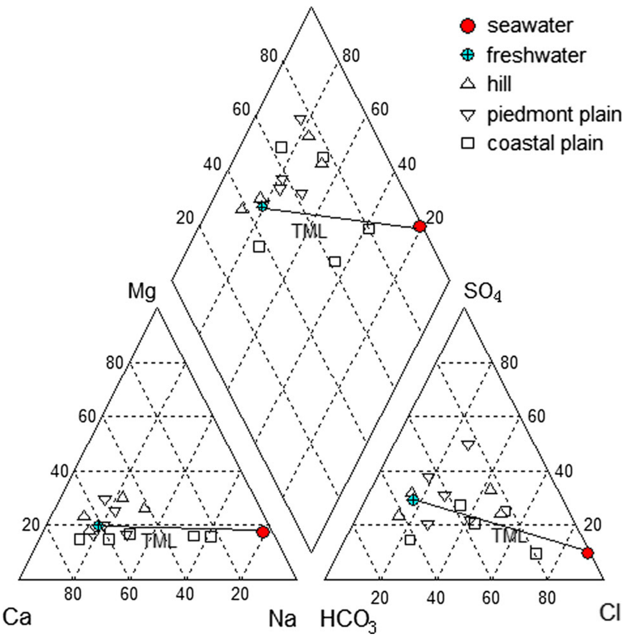

Fig. 3 Piper diagram of groundwater samples

The water quality of each sample was plotted on a classical Piper diagram (Fig. 3). Different groundwater types were observed in the hills, the piedmont plain and the coastal alluvial plain. Ca·Mg–Cl·SO_4 and Ca·Mg–HCO_3-SO_4 type water were found in the hills, Ca·Mg–HCO_3·SO_4 and Ca·Na–HCO_3·Cl in the piedmont plain and Na–Cl in the coastal alluvial plain. The groundwater showed a hydrochemical evolution from Ca·Mg–HCO_3·SO_4 type via Ca·Na–HCO_3·Cl type to Na–Cl type. The piper diagram shows that a few of samples plot near the theoretical mixing line (TML) in the piedmont plain and the coastal alluvial plain, indicating that mixing processes between seawater and freshwater were taking place. Other samples deviated from the TML due to their higher SO_4^{2-} and Ca^{2+} contents. The most likely source of the sulfate is from dissolution of small amounts of gypsum scattered through the aquifer (Kouzana et al. 2009). Calcium may stem from the dissolution of calcite (Pulido-Leboeuf 2004). Thus, simple mixing, ion exchange, minerals dissolution might occur simultaneously in the aquifer system.

The characteristics of groundwater salinity

The salinity of the groundwater is determined by EC (Bouchaou et al. 2008; Giménez and Morell 1997), which was chosen as an index to evaluate the extent of groundwater salinity (Fig. 4). The main contributors to the groundwater salinity are Cl^-, Na^+, Mg^{2+}, Ca^{2+}, K^+, SO_4^{2-}, HCO_3^- and NO_3^-, all of which occurred in concentrations (4.86, 4.08, 2.69, 6.16, 0.17, 2.52, 1.75 and 3.40 meq/L, respectively). EC values in the groundwater ranged from 322 to 3990 µS/cm, with an average of 1240 µS/cm. The highest values were measured in the coastal alluvial plain and in the hills. The high concentrations in the coastal alluvial plain are the results of seawater intrusion into the aquifer system from the eastern boundary of the study area, and the other high ones in the hills stem from human activities such as agriculture, industry. Also, there are many wells which receive pollution from domestic and animal effluents.

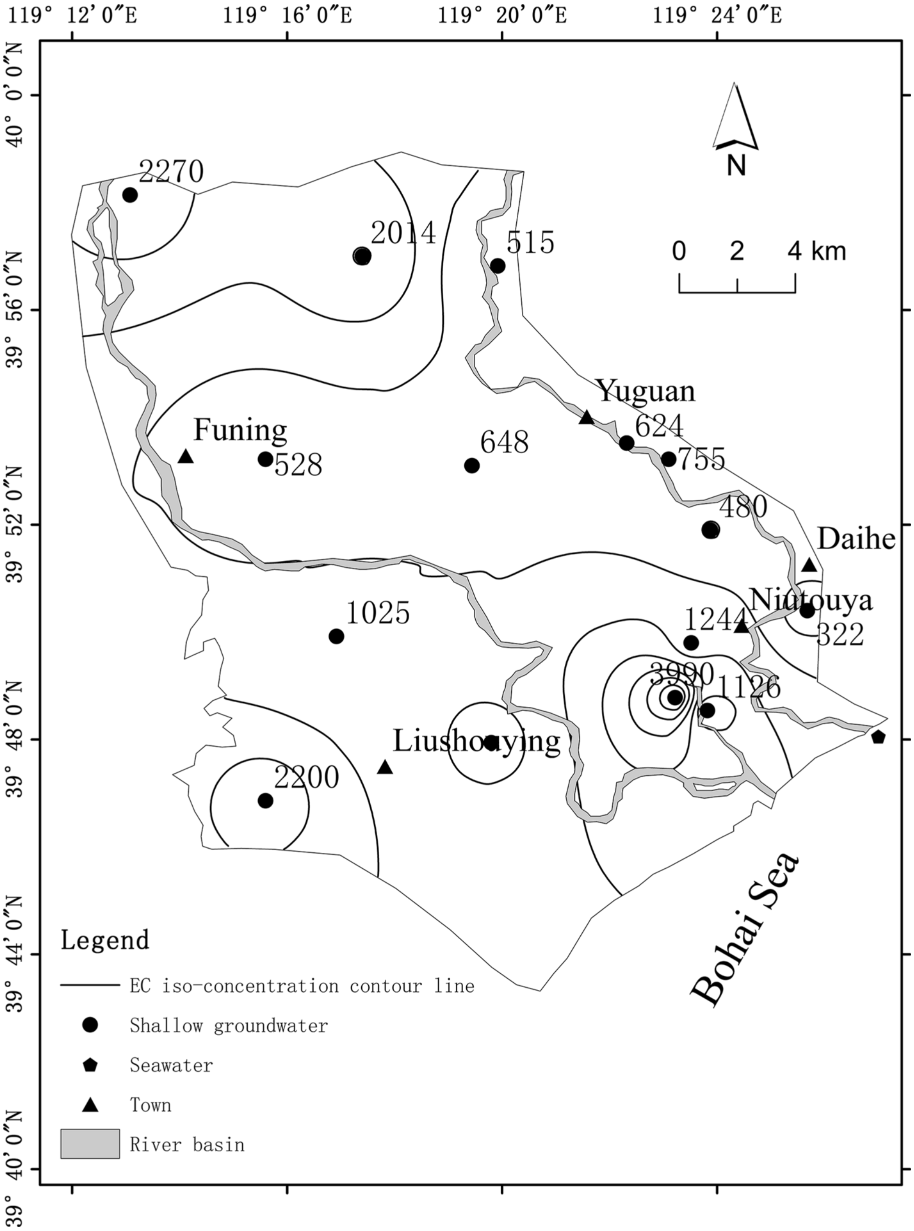

Fig. 4 Spatial distributions of electric conductivity (EC)

Discussion

Seawater intrusion processes

The extent of seawater intrusion is shown in Fig. 5a, b. The trend of the chloride distribution is consistent with the seawater fraction. The most serious seawater intrusion area is located in the coastal alluvial plain with a chloride concentration of 942 mg/L and a seawater proportion of 5.39 %. The drawdown from excessive exploitation of groundwater has led to seawater intrusion, and the most serious intrusion area is close to the previous Zaoyuan water source area (Zuo 2006). In the hills, the chloride concentration was up to 291 mg/L and the seawater proportion of 1.59 %, where values are higher than in the piedmont plain due to evaporation, halite dissolution and the use of chlorine-containing fertilizers.

Ions behave differently under the effect of seawater intrusion (de Montety et al. 2008). Therefore, a series of ionic ratio plots can explain the origin and the processes of groundwater salinization. If simple mixing between seawater and fresh groundwater takes place, there will be a perfectly linear relationship between the electrical conductivity and the chloride concentration (Milnes et al. 2006). The bivariate diagram (Fig. 6a) reveals good correlation for most samples between the electrical conductivity and the chloride concentration. Most samples scatter around the mixing line. Part of the samples are located in the chloride-enriched domain (below the mixing line), which suggests possible chloride sources from other salinization processes such as the dissolution of halite.

Figure 6b shows the relationship between sodium and chloride. The samples also distribute around the mixing line. Few samples below the mixing line indicate that sodium is depleted in the aquifer. However, almost all samples (Fig. 6c) concentrated in the calcium enrichment domain. According to Fig. 6d, Mg^{2+} concentrations change distinctly at different points. The depletions of Na^{+}, and the corresponding enrichment in Ca^{2+} and Mg^{2+} at some points, suggest cation-exchange reactions and a strong water–rock interaction related to dilution of gypsum, dolomite and calcite. The trend of Mg^{2+} is consistent with the trend of $SO_4{}^{2-}$ (Fig. 6e).

In order to completely understand the processes that the theoretical content variation indicates, and to find out more about the behavior of the cations, the ionic delta was

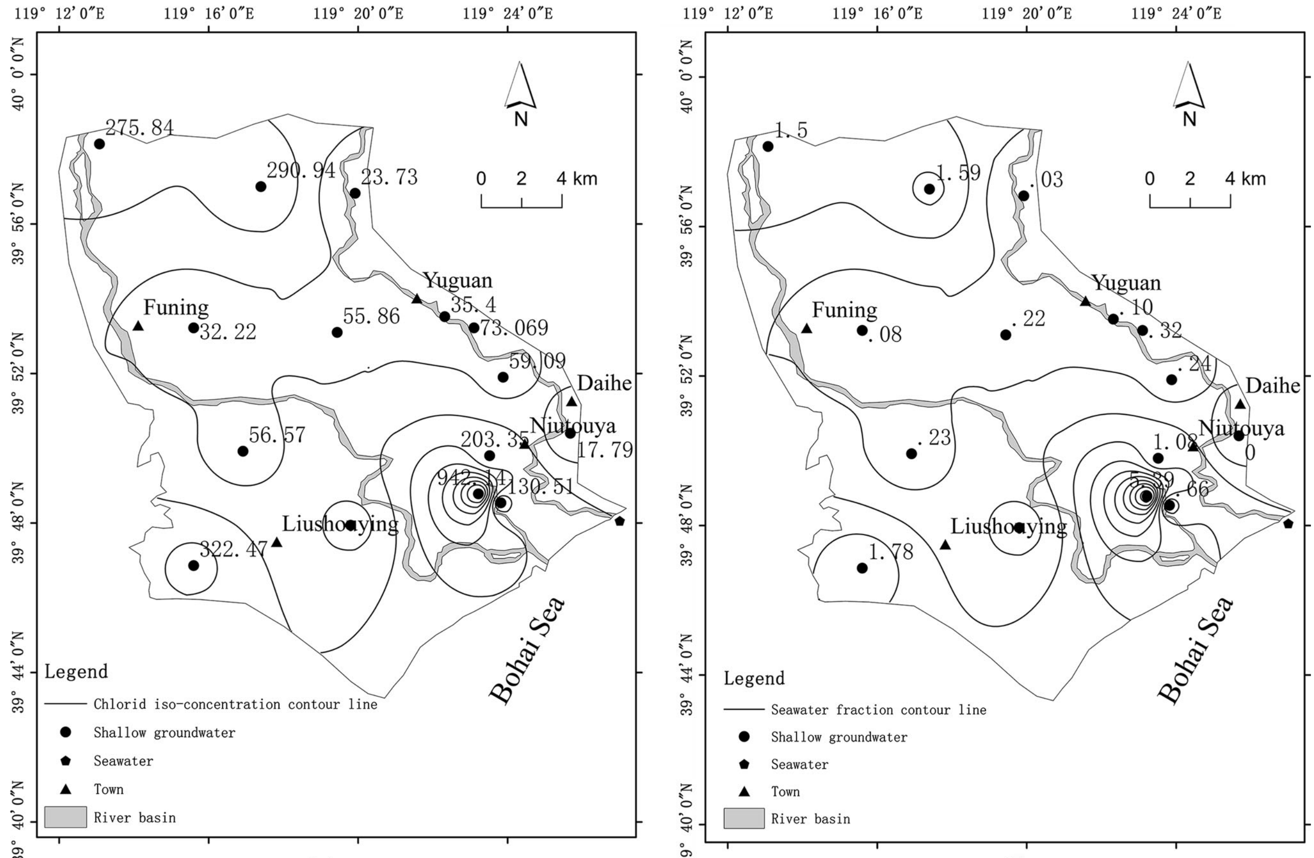

(a) (b)

Fig. 5 Spatial distributions of: **a** chloride concentration, **b** seawater percentage

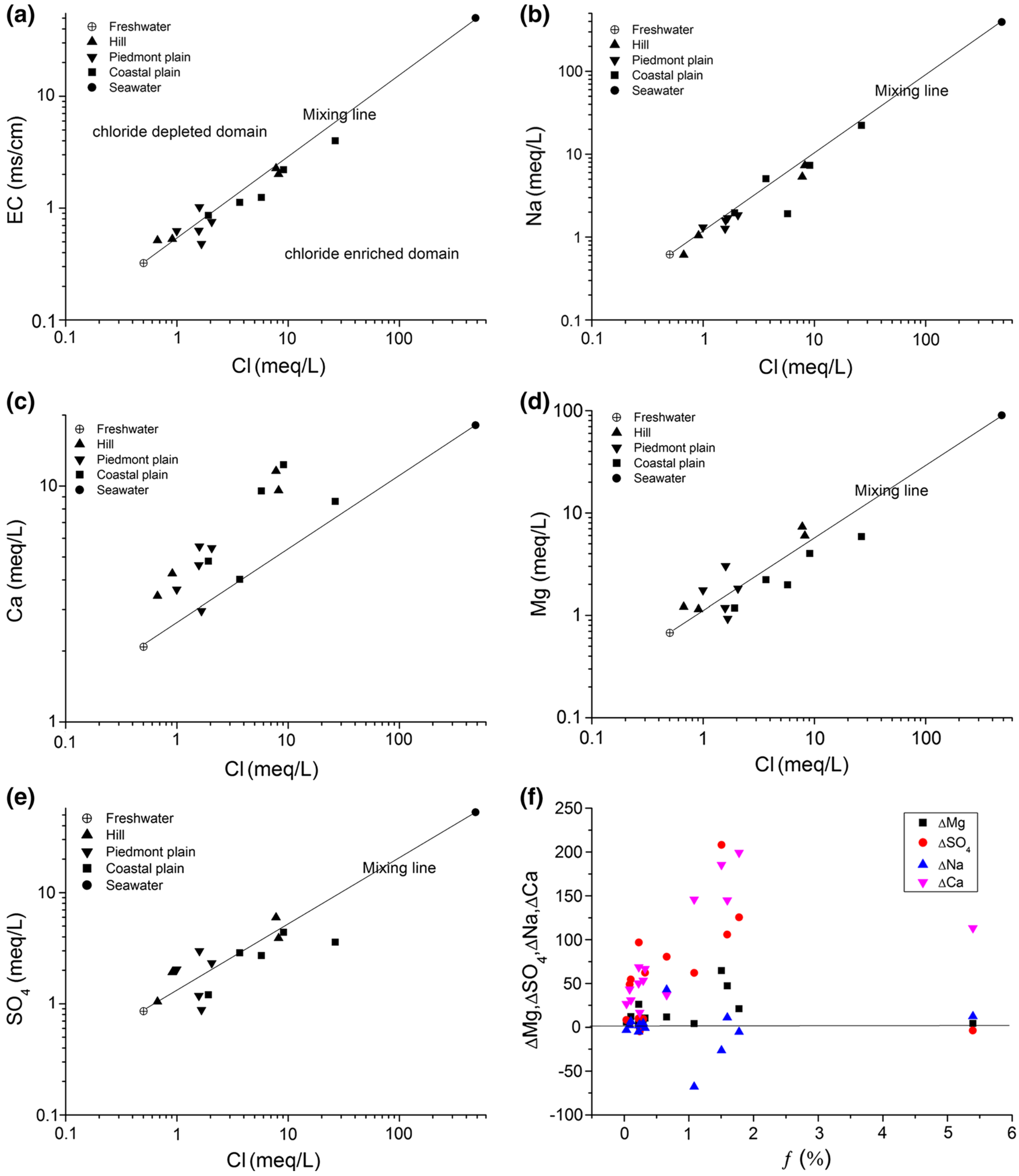

Fig. 6 The bivariate diagram: **a** electrical conductivity/Cl relationship, **b** Na/Cl relationship, **c** Ca/Cl relationships, **d** Mg/Cl relationships, **e** SO_4/Cl relationships, **f** Na, Ca, Mg and SO_4 versus seawater percentage of groundwater samples

plotted for sodium, calcium, magnesium and sulfate (Fig. 6f). The great majority of the samples are depleted in Na^+ and enriched in Ca^{2+}, Mg^{2+} and SO_4^{2-}. This also suggests a direct cation exchange as it usually happens in the initial stage of seawater intrusion (El Yaouti et al. 2009) and the dilution of gypsum, dolomite and calcite. However, the excess of Ca^{2+}, Mg^{2+} and SO_4^{2-} indicates the existence of other sources contributing to the enrichment of groundwater. Fertilizers can be considered as potential sources of Ca^{2+}, Mg^{2+} and SO_4^{2-} (Milnes and Renard 2004).

Pollution by human activities

Due to the joint development of industry, agriculture and tourism, groundwater is under enormous pressure in the study area. Contamination by nitrate occurred. The spatial distribution of the nitrate pollution is shown in Fig. 7.

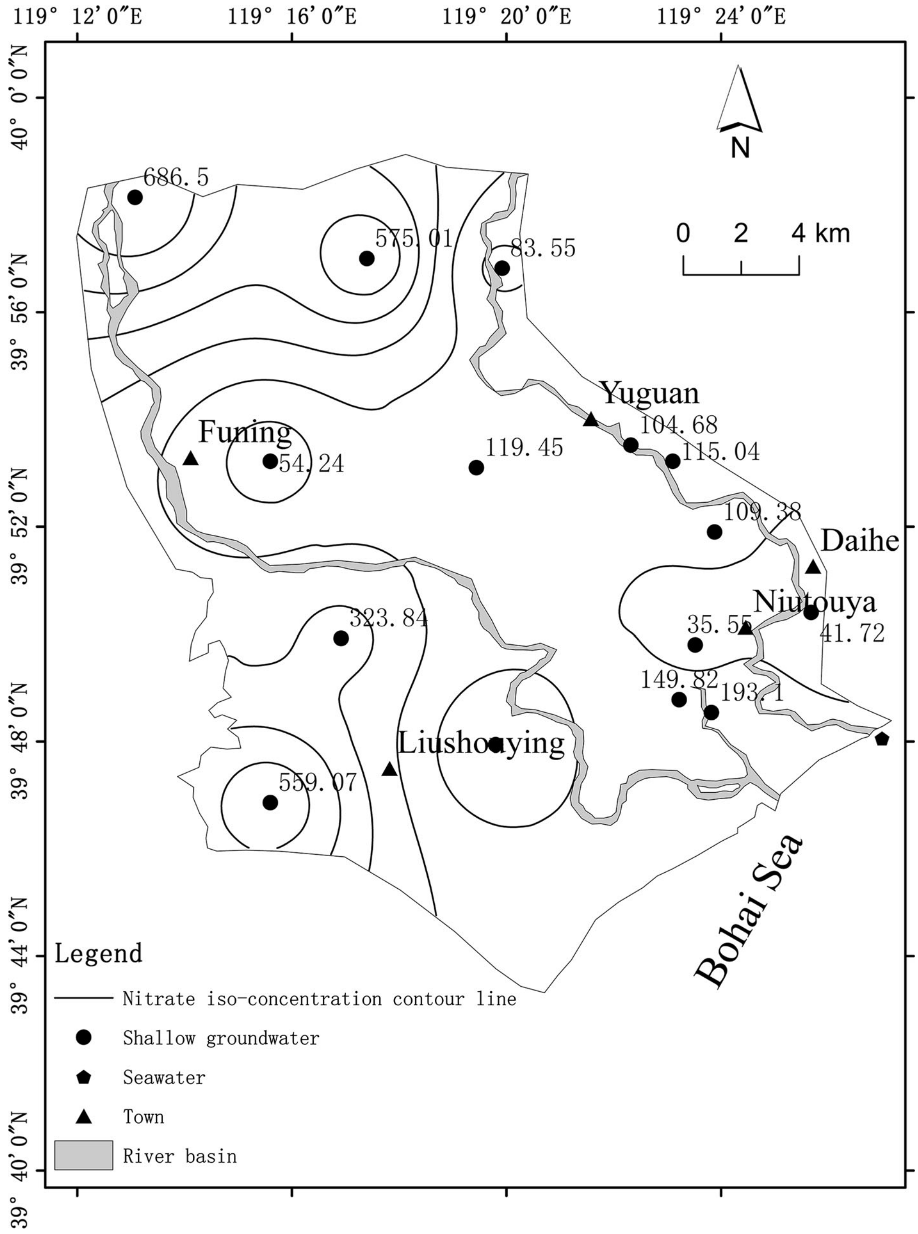

Fig. 7 Spatial distributions of nitrate (NO_3)

Nitrate concentrations range between 35.6 and 686.5 mg/L. The majority of the study area is subjected to pollution above the drinking water standard (50 mg/L). The most serious polluted areas are concentrated in the hills and in the south coastal of the alluvial plain. Agriculture is the dominant land-use form in the hills, and lots of fertilizers with high level of NO_3^- flow into groundwater. In the south coastal alluvial plain, nitrate concentration increased due to industrial wastewater, fertilizers and domestic sewage.

The relationship between nitrate contamination and seawater intrusion is shown in Fig. 8a, which reveals high nitrate concentrations at low seawater fraction. This indicates that the nitrate contamination has no relation to seawater intrusion. Instead, nitrate contamination can be attributed to human activities including abuse of fertilizer, industrial wastewater and domestic sewage.

In the case of contamination by nitrate, the ratio NO_3^-/Cl^- versus Cl^- (Fig. 8b) can be used as an indicator to identify seawater mixing and anthropogenic pollution (Park et al. 2005). A NO_3^-/Cl^- ratio close to 0 suggests a high extent of seawater intrusion (Khaska et al. 2013; Zghibi et al. 2013). Reversely, a high ratio indicates pollution by human activities. Obviously, there are two group samples in Fig. 8b. A part of samples indicate not only seawater intrusion, but also nitrate contamination, which is located in the south coastal alluvial plain.

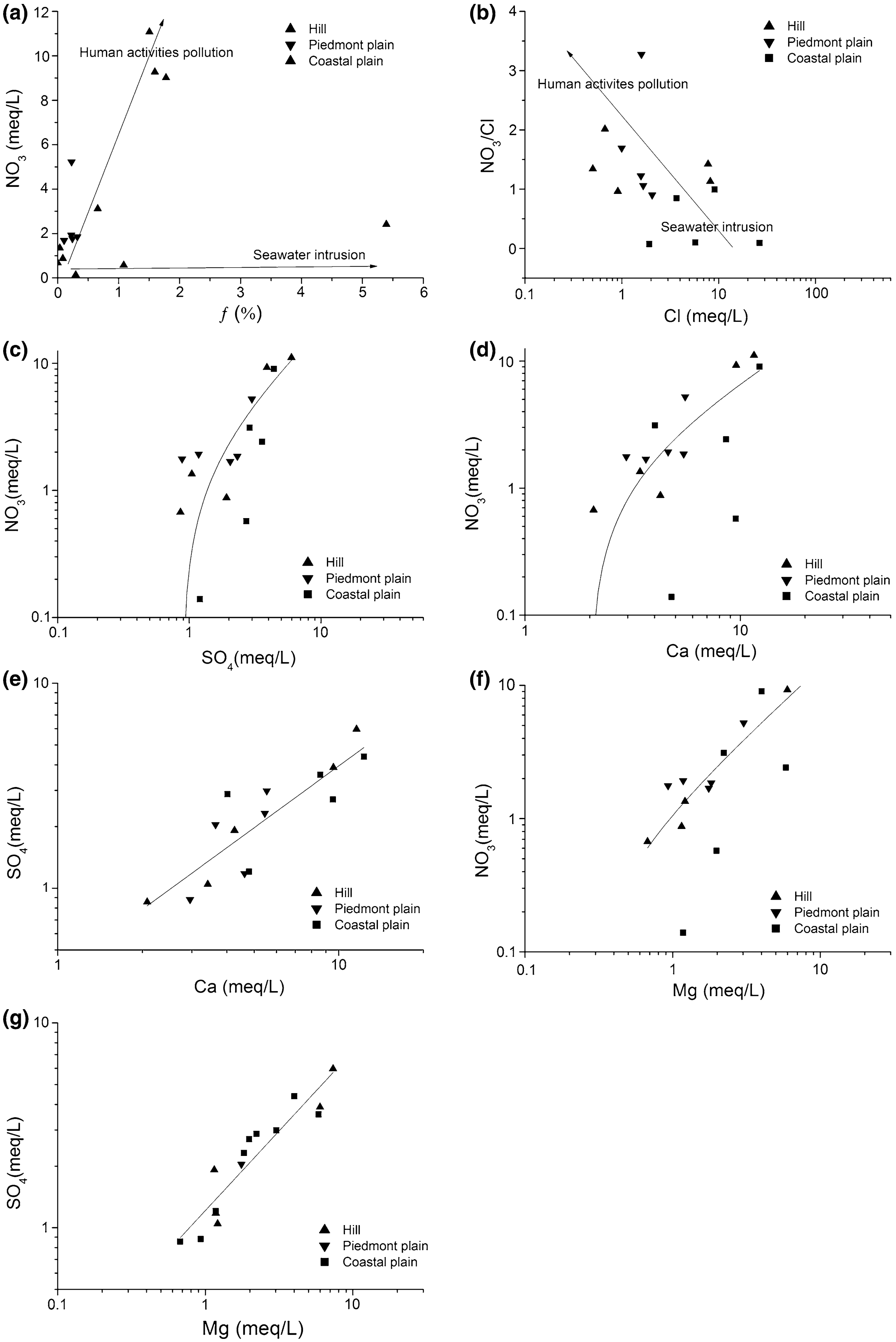
(a)
Human activities pollution
Seawater intrusion
Hill
Piedmont plain
Coastal plain
NO3 (meq/L)
f (%)
0
2
4
6
8
10
12
0
1
2
3
4
5
6
(b)
Human activites pollution
Seawater intrusion
Hill
Piedmont plain
Coastal plain
NO3/Cl
Cl (meq/L)
0
1
2
3
4
0.1
1
10
100
(c)
Hill
Piedmont plain
Coastal plain
NO3(meq/L)
SO4(meq/L)
0.1
1
10
(d)
Hill
Piedmont plain
Coastal plain
NO3(meq/L)
Ca (meq/L)
0.1
1
10
(e)
Hill
Piedmont plain
Coastal plain
SO4(meq/L)
Ca (meq/L)
1
10
(f)
Hill
Piedmont plain
Coastal plain
NO3(meq/L)
Mg (meq/L)
0.1
1
10
(g)
Hill
Piedmont plain
Coastal plain
SO4(meq/L)
Mg (meq/L)
0.1
1
10

◀ **Fig. 8** The bivariate diagram: **a** seawater fraction versus NO_3, **b** chloride versus NO_3/Cl, **c** SO_4/NO_3 relationship, **d** Ca/NO_3 relationship, **e** Ca/SO_4 relationship, **f** Mg/NO_3 relationship, **g** Mg/SO_4 relationship for groundwater samples

The plot of SO_4^{2-} versus NO_3^- (Fig. 8c) exhibits a certain relationship, which indicates an origin of $SO_4^{2-}$and NO_3^- related to either gypsum dissolution or by the contribution of SO_4^{2-} fertilizers (Chae et al. 2004). The same situation appeared in Fig. 8d, which shows a certain relationship between Ca^{2+} and NO_3^-, suggesting the origin of Ca^{2+} is both dissolution of gypsum (dolomite, calcite) and application of $Ca(NO_3)_2^-$ fertilizers (Ben Moussa et al. 2008; Stigter et al. 2006). Therefore, salinization is not only due to typical seawater ions but also due to those elements contained in fertilizers like NO_3^-, $SO_4^{2-}$and Ca^{2+} that increase EC value.

Conclusion

A series of methods were used to study the origin of groundwater salinity and hydrochemical processes including ion spatial distribution, ionic deviations, piper diagram, seawater fractions and binary plots. It was found that the water type varies in different places: $Ca{\cdot}Mg–Cl{\cdot}SO_4$-type water was identified in the hilly areas, $Ca{\cdot}Mg–SO_4{\cdot}Cl$ identified in the piedmont plain, and Na–Cl dominated in the coastal alluvial plain.

EC values varied between 322 and 3990 µS/cm, with an average of 1240 µS/cm. Higher values were found in the coastal alluvial plain and in the hills than in piedmont plain. Groundwater salinization is caused by typical seawater intrusion and anthropogenic pollution by NO_3^-. The most serious seawater intrusion area is located in the coastal alluvial plain with a chloride concentration up to 942 mg/L and a chloride proportion of 5.39 %. Ion behaviors suggest that cation-exchange reactions and strong water–rock interactions related to dilution of halite, gypsum, dolomite and calcite happened during seawater intrusion.

Nitrate concentrations were found to be above the drinking water standard (50 mg/l) in most of the study area and varied between 35.6 and 686.5 mg/L. The hills and the south coastal alluvial plain suffered from severe pollution from industrial wastewater, fertilizers and domestic sewage. A part of the samples indicated simultaneous seawater intrusion and nitrate contamination, mostly located in the south of the coastal alluvial plain. Accordingly, the groundwater salinization seems to be a complex process with two main sources, seawater intrusion and anthropogenic pollution.

Acknowledgments This work was supported by the "Groundwater-environment-social economy coupling mechanism and evaluation system in China" (Project No. 2010CB428805). The authors express their sincere gratitude to Bing Zhang and Xiangmin Sun for their assistance during the fieldwork.

References

Andersen MS, Nyvang V, Jakobsen R, Postma D (2005) Geochemical processes and solute transport at the seawater/freshwater interface of a sandy aquifer. Geochim Cosmochim Acta 69:3979–3994. doi:10.1016/j.gca.2005.03.017

Appelo CAJ, Postma D (2005) Geochemistry, groundwater and pollution, seconded. Balkema, Rotterdam

Bouchaou L et al (2008) Application of multiple isotopic and geochemical tracers for investigation of recharge, salinization, and residence time of water in the Souss–Massa aquifer, southwest of Morocco. J Hydrol 352:267–287. doi:10.1016/j.jhydrol.2008.01.022

Chae GT et al (2004) Hydrogeochemistry of alluvial groundwaters in an agricultural area: an implication for groundwater contamination susceptibility. Chemosphere 55:369–378. doi:10.1016/j.chemosphere.2003.11.001

Custodio E, Bruggeman GA (1987) Hydrogeochemistry and tracers. In: Custodio E (ed) Groundwater problems in coastal areas studies and reports in hydrology, vol 45. UNESCO, Paris, pp 213–269

de Montety V, Radakovitch O, Vallet-Coulomb C, Blavoux B, Hermitte D, Valles V (2008) Origin of groundwater salinity and hydrogeochemical processes in a confined coastal aquifer: case of the Rhône delta (Southern France). Appl Geochem 23:2337–2349. doi:10.1016/j.apgeochem.2008.03.011

El Yaouti F, El Mandour A, Khattach D, Benavente J, Kaufmann O (2009) Salinization processes in the unconfined aquifer of Bou-Areg (NE Morocco): a geostatistical, geochemical, and tomographic study. Appl Geochem 24:16–31. doi:10.1016/j.apgeochem.2008.10.005

Giménez E, Morell I (1997) Hydrogeochemical analysis of salinization processes in the coastal aquifer of Oropesa (Castellon, Spain). Environ Geol 29:118–131

Han Z (1990) Controlling and harnessing of the sea water intrusion in the alluvial plain of Yang River and Dai River in Qinhuangdao. Geoscience 4:105–115

Khaska M et al (2013) Origin of groundwater salinity (current seawater vs. saline deep water) in a coastal karst aquifer based on Sr and Cl isotopes. Case study of the La Clape massif (southern France). Appl Geochem 37:212–227. doi:10.1016/j.apgeochem.2013.07.006

Kouzana L, Mammou AB, Felfoul MS (2009) Seawater intrusion and associated processes: case of the Korba aquifer (Cap-Bon, Tunisia). CR Geosci 341:21–35. doi:10.1016/j.crte.2008.09.008

Mahesha A, Nagaraja SH (1996) Effect of natural recharge on sea water intrusion in coastal aquifers. J Hydrol 174:211–220

Milnes E, Renard P (2004) The problem of salt recycling and seawater intrusion in coastal irrigated plains: an example from the Kiti aquifer (Southern Cyprus). J Hydrol 288:327–343. doi:10.1016/j.jhydrol.2003.10.010

Milnes E, Meilhac C, Yeo D, Renard P, Hunkeler D, Schnegg P, Bourret F (2006) Hydrogeochemical and hydrogeological investigation in the Akrotiri aquifer: identification of multiple salinisation processes and implementation criteria for monitoring networks. SWIM-SWICA

Moussa AB, Zouari K, Oueslati N (2008) Geochemical study of groundwater mineralization in the Grombalia shallow aquifer, north-eastern Tunisia: implication of irrigation and industrial waste water accounting. Environ Geol 58:555–566. doi:10.1007/s00254-008-1530-7

Park S-C, Yun S-T, Chae G-T, Yoo I-S, Shin K-S, Heo C-H, Lee S-K (2005) Regional hydrochemical study on salinization of coastal aquifers, western coastal area of South Korea. J Hydrol 313:182–194. doi:10.1016/j.jhydrol.2005.03.001

Pulido-Leboeuf P (2004) Seawater intrusion and associated processes in a small coastal complex aquifer (Castell de Ferro, Spain). Appl Geochem 19:1517–1527. doi:10.1016/j.apgeochem.2004.02.004

Slama F, Bouhlila R, Renard P (2010) Identification of groundwater salinization sources using experimental, multivariate statistical analysis and numerical modelling tools: case of Korba coastal aquifer (Tunisia). In: XXXVIII IAH congress, groundwater quality sustainability, Krakow, 12–17 Sept

Steinich B, Escolero O, Marín LE (1998) Salt-water intrusion and nitrate contamination in the Valley of Hermosillo and El Sahuaral coastal aquifers, Sonora, Mexico. Hydrogeol J 6:518–526

Stigter TY, Dill AMMC, Ribeiro L, Reis E (2006) Impact of the shift from groundwater to surface water irrigation on aquifer dynamics and hydrochemistry in a semi-arid region in the south of Portugal. Agric Water Manag 85:121–132. doi:10.1016/j.agwat.2006.04.004

Trabelsi R, Zairi M, Dhia HB (2007) Groundwater salinization of the Sfax superficial aquifer, Tunisia. Hydrogeol J 15:1341–1355. doi:10.1007/s10040-007-0182-0

Xiao G, Yang J, Hu Y, Du D (2014) Hydrogeochemical recognition of seawater intrusion processes in Yang River and Dai River coastal plain of Qinhuangdao City. Saf Environ Eng 21:30–39

Zghibi A, Tarhouni J, Zouhri L (2013) Assessment of seawater intrusion and nitrate contamination on the groundwater quality in the Korba coastal plain of Cap-Bon (North-east of Tunisia). J Afr Earth Sc 87:1–12. doi:10.1016/j.jafrearsci.2013.07.009

Zhang B (2012) Mechanism of seawater intrusion using hydrochemistry and environmental isotopes in Qinhuangdao Yang Dai Master thesis

Zhang B, Song X, Guo Z, Zhao X (2013) Investigation of the origin and evolution of groundwater in Yang-Dai River Plain by chlorine, oxygen 18 and deuterium. Acta Clientage Circumstantiate 33:2965–2972

Zuo W (2006) Survey and research on seawater intrusion in the Yandaihe Plain of Qinhuangdao City doctoral thesis

Zuo W, Yang Y, Dong Y, Liang M (2009) The numerical study for seawater intrusion in Yanghe and Daihe Coastal Plain of Qinhuangdao City. J Nat Resour 24:2087–2209